Research Article

SCHIFF BASE COMPLEXES OF TITANOCENE DICHLORIDE: SYNTHESIS, CHARACTERIZATION, DFT MODELING, ANTIBACTERIAL AND CATALYTIC ACTIVITY

Satyendra N. Shukla, Pratiksha Gaur, Dimple Dehariya, Bhaskar Chaurasia
Coordination Chemistry Research Lab, Department of Chemistry, Government Science College, Jabalpur (M.P.) 482001, INDIA
Author for Correspondence: ccrl_2004@rediffmail.com

ABSTRACT

This manuscript deals with the synthesis of titanocenedichloride complexes with Schiff base ligands derived from the condensation of 1, 3-diamino propane with 2-hydroxyacetophenone/salicyl aldehyde/*p*-chlorobenzaldehyde. The ligands and complexes were characterized by analytical technique *viz.* elemental analysis, molar conductance, magnetic suceptibility and spectroscopic technique *viz.* FT-IR, UV-VIS, ESI-Mass, ^{1}H-NMR and ^{13}C-NMR spectroscopy. In order to assign the structure of compounds computational studies were performed using DFT calculations at B3LYP/6-311+G(d,p) and LANL2DZ level of theory. Additionally, molecular electrostatic potential map (MEP), HOMO, LUMO and Mullikan charge analysis were also done. Spectroscopic chracterization and DFT study proposed a distorted octahedral structure of complex **1-5**. Complexes were screened for catalytic activity in ring opening polymerization of ε-caprolactone. Number average molecular weight (M_n) of resulting polycapralactone was calculated using viscosity method.

Keywords: Schiff Base Ligand; Catalytic Activity; DFT Study; Corrosion inhibition; Antibacterial Activity

INTRODUCTION

In the last decade, Schiff base ligands have received more attention mainly because of their wide spread application in the field of catalysis, (Halpern 1965) anticorrosion, (Mishra *et al.,* 2015) and antibacterial activity.(Azam *et al.,* 2018). They are a class of ligands, well known to coordinate with transition metal ions through the azomethine nitrogen to form stable complexes (Joshi *et al.*2011). Substituted cyclopentadienes as ligands for group IV metallocene are still one of the important subjects of organometallic chemistry (Janiak and Schumann1991). The derivatives of titanocene dichloride with SALEN type ligands exhibit good biological activity. (Kumar and Chandra 2011). Some titanocene dichloride complexes were active toward cisplatin resistant tumor cells, while demonstrating reduced side effects.

In chemical industry, there is always a search for effective, highly selective and environmentally safe catalysts and titanium complexes are one of the most active early catalyst frame works of metallocene system (Bhattacharjee and Patra 2004). Several titanocene complexes give dimers with two *bis*-cyclopentadienyl titanium(IV) units connected *via* oxygen bridging [(Cp$_2$TiCl)$_2$O] (Erben *et al.,* 2009). The objectives of this study were to evaluate the corrosion resistance of various surface structures in the most prevalent implants-titanium, and determined the changing situation of corrosion. The corrosion parameters of them were used to comparing the corrosion resistance of different samples. In view of the above facts, it will be interesting to prepare Schiff base ligands by condensation of 2-hydroxyacetophenone/ salicylaldehyde/ *p*-chlorobezaldehyde with 1,3-diaminopropane linker and to derive its *bis*-cyclopentadienyl titanium (II) complexes. The resulting ligands and complexes will be characterized by the spectroscopic methods (Honzicek *et al.,* 2004). In anticipation of good catalytic and biological activity, complexes will also be screened for their catalytic activity of ring opening polymerisation of ε-caprolactone and antibacterial activity. However, since DFT is a simulated quantum

Research Article

mechanical calculation technique which provides information about compounds before its synthesis in the lab, we are also interested in optimizing the structure of the resulting ligand and complexes by DFT.

MATERIALS AND METHODS

All the chemicals and solvents used throughout experiment were of A.R. grade. 1,3-diaminopropane, 2-hydroxyacetophenone, salicylaldehyde, *p*-chlorobenzaldehyde, $(\eta^5-C_5H_5)_2TiCl_2$, (All E. Merck). AR grade acetone, DMSO (E. Merck), Mueller Hinton Agar media (Himedia) were used as received. Solvent ethanol and methanol were used after double distillation. Elemental analysis was estimated on Euro Vector E-3000 elemental analyzer and metal content was analyzed gravimetrically by the literature procedure (Jeffery *et al.* 1989). Conductivity measurements were carried out in DMSO at 25 °C on an EI-181 conductivity bridge with dipping type cell. ESI-MS spectra were recorded on Agilent - 6520(Q-TOF) mass spectrometer. FT-IR spectra were recorded in KBr pellets on Shimadzu-8400 PC spectrometer. Electronic absorption spectra were recorded in the range 800-200 nm with an EI-2371 double beam spectrophotometer equipped with a PC. ^{1}H-NMR and the ^{13}C-NMR spectrum were recorded in DMSO-d_6 on a Bruker Avance 400 (FT-NMR) spectrophotometer at 400 MHz.

Preparation of ligands

Synthesis of Schiff base ligand (3E,4E)-N^1,N^3-bis(1-methyl-2-hydroxybenzylidene)propane-1,3-propylenediamine; L$_1$

The ligand L$_1$ was prepared by the method reported in literature (Ibrahim and Etaiw 2004). 2-Hydroxyacetophenone (2.40 mL, 0.02 mol) dissolved in 20 mL ethanol was added to 20 mL ethanoic solution of 1,3-diaminopropane (0.83 mL, 0.01 mol). The reaction mixture was refluxed for 20 h. A dark orange precipitate was obtained, which was filtered, dried in vacuum and recrystallized from hot methanol to obtain dark orange shining crystal. Colour = Dark orange, Yield: 2.395 g (74%); m. p. = 110 °C; Analysis Calcd. for $C_{19}H_{22}N_2O_2$ (310.39): C, 73.52; H, 7.14; N 9.03. Found: C, 73.42; H 7.10; N 8.91. Selected infrared absorption (KBr, cm^{-1}): 3356 ν(O-H), 1615 ν(HC=N) . Electronic spectra (λ$_{max}$ in nm, ε in M^{-1}cm^{-1}) in DMF: 240 (720), 300 (1675). ^{1}H-NMR spectra (δ value in ppm): δ(O-H) 14.348(s, 2H), δ(Ar-H) 6.777(m, 4H), 7.279(t, 2H, 18Hz, 20Hz), 7.637(d, 2H, 20Hz), δ(CH$_2$) 3.686(t, 6H), δ(-CH$_3$) 2.044(s, 6H). ^{13}C-NMR spectra (δ value in ppm): δ(>C=N)$_{imine}$,163.80, δ(C-OH),172.82; δ(Ar-C),116.48-132.35, δ(-CH$_3$),14.28, δ(-CH$_2$), 46.13. ESI-Mass spectra, m/z: $[C_9H_{10}NO + H^+]^+$ = 149.0796, $[C_{10}H_{12}NO+ H^+]^+$ = 163.09, $[C_{11}H_{14}NO + H]^+$ = 177.11, $[C_{13}H_{17}N_2O + H]^+$ = 218.13, $[C_{19}H_{22}N_2O_2 + H^+]^+$= 311.17, Mτ = 310. 17.

Synthesis of Schiff base ligand Synthesis (3E,4E)-N^1,N^3-bis(salcylidene)-1,3 propylenediamine, L$_2$

Salicylaldehyde (2.13 mL, 0.02 mol) and 1,3-diaminopropane (0.83 mL, 0.01 mol) were mixed in 40 mL ethanol. The reaction mixture was stirred for 4 h and refluxed for 25 h. A yellow precipitate was obtained, which was filtered, dried in vacuum and recrystallized from hot methanol to obtain yellow shining crystal. Colour = yellow, Yield: 2.130 g (72%); m. p. = 110 °C; Anal. Calcd. for $C_{17}H_{18}N_2O_2$ (282.33): C, 72.32; H, 6.43; N 9.92. Found: C, 73.22; H 6.35; N 9.81. Selected infrared absorption (KBr, cm^{-1}): 3352; ν(O-H), 1619 ν(HC=N). Electronic spectra (λ$_{max}$ in nm, ε in M^{-1}cm^{-1}) in DMF: 235 (680), 290 (1655). ^{1}H-NMR spectra (δ value in ppm, 300 K): δ(O-H)$_{phenol}$, 12.154 (s, 2H); δ(-HC=N), 8.568(s, 2H), (Ar-H), 6.648(t, 2H), 7.185(t, 2H), 7.506(d, 2H), 7.486(d, 2H), δ(CH$_2$), 3.634(m, 6H). ^{13}C-NMR spectra (δ value in ppm): δ(>C=N)$_{imine}$,162.84, δ(C-OH),170.89; δ(Ar-C), 116.52-148-58, δ(-CH$_2$), 43.06. ESI-Mass spectra, m/z: $[C_9H_{10}NO]^+$ = 148.0762; $[C_{10}H_{12}NO + H]^+$ = 163.0919, $[C_{11}H_{13}N_2O + H]^+$ = 190.1023, $[C_{17}H_{18}N_2O_2+ H^+]^+$= 283.1368, Mτ= 282.34.

Synthesis of Schiff base ligand(3E,4E)-N^1,N^3-bis(4-chlorobenzylidene) propane-1,3-diamine, L$_3$

4-Chlorobenzaldehyde (2.81 g, 0.02 mol) and 1,3-diaminopropane (0.83 mL, 0.01 mol) were mixed in 40 mL ethanol. The reaction mixture was stirred for 5 h and refluxed for 20 h. An off white precipitate was obtained, which was filtered, dried in vacuum and recrystallized from hot methanol to obtain off white shining crystal. Colour = off white, Yield: 2.548 g (70%); m. p. = 120 °C; Anal. Calc. for $C_{17}H_{16}Cl_2N_2$

Research Article

(319.22): C, 63.96; H, 5.05; N 8.78. Found: C, 63.86; H 4.95; N 8.67. Selected infrared absorption (KBr, cm^{-1}): 1612 ν(HC=N). Electronic spectra (λ_{max} in nm, ε in M^{-1}cm^{-1}) in DMF: 246 (665), 310 (1670). ^{1}H-NMR spectra (δ value in ppm, 300 K): δ(-HC=N)$_{imine}$ 8.456 (s, 2H), δ(Ar-H) 6.948 (d, 4H), 7.028 (d, 4H), δ(CH$_2$) 3.302 (m, 6H). ^{13}C-NMR spectra (δ value in ppm): δ(-CH=N)$_{imine}$, 162.84, δ(Ar-C) 115.50-140.38, δ(-CH$_2$) 44.92. ESI-Mass spectra, m/z: [C$_8$H$_7$ClN + H]$^+$ = 153.04, [C$_9$H$_9$ClN + H]$^+$ = 167.0424, [C$_{10}$H$_{11}$ClN + H]$^+$ = 181.0580, [C$_{11}$H$_{12}$ClN$_2$ + H]$^+$ = 208.0689, [C$_{17}$H$_{16}$ClN$_2$ + H]$^+$ = 284.12, [C$_{17}$H$_{16}$Cl$_2$N$_2$+ H$^+$]$^+$ = 319.0691, Mτ= 318.06.

Preparation of complexes

Synthesis of complexes [(cp)$_2$Ti(L$_1$)]Cl; 1

Ligand **L$_1$** (0.31 g, 0.01 mol) and bis(cyclopentadienyl)titanocenedichloride(0.24 g, 0.01 mol) were mixed in 40 mL of (1:1, v/v) of methanol and acetone. The reaction mixture was kept under stirring for 1 h in an inert atmosphere. The colour of reaction mixture changes from dark red to reddish brown. Thereafter, reaction mixture was refluxed for 13 h. After slow evaporation of the solution a black solid was obtained, which was filtered and dried in vacuum. Solid obtained was recrystallized from methanol: acetone, 1: 2 solvent mixture (v/v). Colour = black, Yield: 0.362 g (65%); m. p. > 300 °C; Anal. Calc. for C$_{31}$H$_{37}$ClN$_2$O$_2$Ti (552.958): C, 67.33; H, 6.74; N 5.07; Ti, 8.66. Found: C, 67.23; H 6.64; N 4.97; Ti, 8.56. μ_{eff} = 2.61 BM. Molar conductance Λm at 25 °C (Ω^{-1} cm^2 mol^{-1}): 29 in DMSO. Selected infrared absorption (KBr, cm^{-1}): 3321 ν(O-H), 1609(s), 1639 ν(HC=N), 510 ν(M-O), 490 ν(M-N). Electronic spectra (λ_{max} in nm, ε in M^{-1}cm^{-1}) in DMF: 300 (690), 340 (1675). ^{1}H-NMR (δ value in ppm): δ(CH=N) 8.274(s, 1H), δ(Ar-H)7.45, 7.12, 6.85, 6.75(m, 5H), 5.00 (s, 2H), δ(-CH$_3$) 3.554(q, 4H), δ(-CH$_2$), 2.01(t, 2H), ^{13}C-NMR spectra (δ value in ppm): δ(>C=N)$_{imine}$ 160.76, δ(C-O)153.67, δ(Ar-C)$_{phenylene}$,113.54-127.31, δ(Ar-C)$_{phenolic}$ 128.09-153.67, δ(-CH$_3$) 12.31. ESI-Mass spectra, m/z: [C$_{11}$H$_{14}$NO + H]$^+$ = 177.11, [C$_{19}$H$_{21}$N$_2$O$_2$ + 2H]$^+$= 311.16, [C$_{20}$H$_{23}$NOTi + H]$^+$= 342.12, [C$_{31}$H$_{37}$N$_2$O$_2$Ti]$^+$ = 517.50 [C$_{31}$H$_{37}$ClN$_2$O$_2$Ti + H]$^+$ = 553.90, M τ = 552.20.

Synthesis of complexes [(cp)$_2$Ti(L$_2$)]Cl; 2

Ligand **L$_2$** (0.28 g, 0.01 mol) and bis(cyclopentadienyl)titanocenedichloride (0.24g, 0.01 mol) were mixed in 50 mL mixture (1:1, v/v) of methanol and acetone. The reaction mixture was kept under stirring for 1 h in an inert atmosphere. The colour of reaction mixture changes from dark red to red brown. Thereafter, reaction mixture was refluxed for 10 h. Dark black solid was obtained after slow evaporation of the solution, which was filtered and dried in vacuum. Solid obtained was recrystallized from methanol: acetone, 1: 2, solvent mixture (v/v). Colour = black, Yield: 0.333 g (63%); m. p. > 300 °C; Anal. Calc. for C$_{29}$H$_{33}$ClN$_2$O$_2$Ti (524.905): C, 66.36; H, 6.34; N 5.34; Ti, 9.12. Found: C, 66.26; H 6.29; N 5.25; Ti, 9.02. μ_{eff} = 2.82 BM. Molar conductance Λm at 25 °C (Ω^{-1} cm^2 mol^{-1}): 28 in DMSO. Selected infrared absorption (KBr, cm^{-1}): 3121 ν(O-H), 1601 ν(HC=N), 518 ν(M-O), 494 ν(M-N). Electronic spectra (λ_{max} in nm, ε in M^{-1}cm^{-1}) in DMF: 290 (680), 335 (1655). ESI-Mass spectra, m/z: [C$_{10}$H$_{12}$NO + H]$^+$= 163.09, [C$_{17}$H$_{17}$N$_2$O$_2$ + H]$^+$= 282.13, [C$_{19}$H$_{27}$NOTi + H]$^+$ = 328.11, [C$_{29}$H$_{33}$N$_2$O$_2$Ti]$^+$ = 489.20, [C$_{29}$H$_{33}$ClN$_2$O$_2$Ti + H]$^+$= 525.17, Mτ = 524.17.

Synthesis of complexes [(cp)$_2$Ti(L$_3$)]Cl; 3

Ligand **L$_3$** (0.33 g, 0.01 mol) and bis(cyclopentadienyl)titanocenedichloride (0.24 g, 0.01 mol) were mixed in 50 mL (1:1, v/v) of methanol and acetone mixture. The reaction mixture was kept under stirring for 1 h in an inert atmosphere. Thereafter, reaction mixture was refluxed for 14 h. Dark black solid was obtained after slow evaporation of the solution, which was filtered and dried in vacuum. Solid obtained was recrystallized from methanol: acetone, 1: 2 solvent mixture (v/v). Colour = black, Yield: 0.351 g (62%); m. p. 300 °C; Anal. Calcd. for C$_{29}$H$_{31}$Cl$_4$N$_2$Ti (597.249): C, 58.32; H, 5.23; N 4.69; Ti, 8.01.

Research Article

Found: C, 58.22; H 5.13; N 4.59; Ti, 7.91. μ_{eff} = 2.78 BM. Molar conductance Λm at 25 °C (Ω^{-1} cm^2 mol^{-1}): 68 in DMSO. Selected infrared absorption (KBr, cm^{-1}): 1606 ν(HC=N), 478 ν(M-N). Electronic spectra (λ_{max} in nm, ε in M^{-1}cm^{-1}) in DMF: 305 (710), 345 (1685). ESI-Mass spectra, m/z: $[C_{17}H_{16}Cl_2N_2 + H^+]^+$ = 319.06, $[C_{29}H_{31}Cl_4N_2Ti]^+$= 561.56, $[C_{29}H_{31}Cl_4N_2Ti + H]^+$ = 598.06, M τ = 597.06.

Synthesis of complexes [(cp)$_4$Ti$_2$(L$_1$)]Cl$_2$; 4
Ligand **L$_1$**(0.31 g, 0.01mol) and bis(cyclopentadienyl)titanocenedichloride(0.49 g, 0.02mol) were mixed in 50 mL 1:2, mixture(v/v)of methanol and acetone. The reaction mixture was kept under stirring for 1 h in an inert atmosphere. Thereafter, reaction mixture was refluxed for 15 h. The colour of reaction mixture changes from dark red brown to black. A black coloured solid was obtained after slow evaporation of the solution which was dried in vacuum. The solid obtained was recrystallized from hot methanol. Colour = Shining black,Yield: 0.556 g (69%); m.p. > 300°C;Analysis Calcd. for C$_{43}$H$_{52}$Cl$_2$N$_2$O$_2$Ti$_2$(795.52): C, 64.92; H, 6.59; N 3.52; Ti 12.03.Found: C, 64.82; H, 6.49; N, 3.42; Ti, 11.93. μ_{eff} = 2.67 BM. Molar conductance Λm at 25 °C (Ω^{-1} cm^2 mol^{-1}): 66 in DMSO. Selected infrared absorption (KBr, cm^{-1}): 1638 ν(HC=N), 511 ν(M-O), 489 ν(M-N). Electronic spectra (λ_{max} in nm, ε in M^{-1}cm^{-1}) in DMF: 295 (695), 350 (1680). ESI-Mass spectra, m/z: $[C_{19}H_{20}N_2O_2 + 3H^+]^+$ = 311.15, $[C_{23}H_{29}NOTi + H^+]^+$= 384.17, $[C_{43}H_{52}N_2O_2Ti_2 + H^+]^+$ = 725.62, $[C_{43}H_{52}ClN_2O_2Ti_2]^+$ = 760.17, $[C_{43}H_{52}Cl_2N_2O_2Ti_2 +H]^+$ = 796.53, Mτ = 795.53.

Synthesis of complexes [(cp)$_4$Ti$_2$(L$_2$)]Cl$_2$; 5
Ligand **L$_2$**(0.28 g, 0.01mol) and bis(cyclopentadienyl)titanocenedichloride(0.49 g, 0.02mol) were mixed in 50 mL 1:2, mixture(v/v)of methanol and acetone. The reaction mixture was kept under stirring for 1 h in an inert atmosphere. The colour of reaction mixture changes from dark red to brown. Thereafter, reaction mixture was refluxed for 15 h. A dark black solid was obtained after slow evaporation of the solution which was dried in vacuum. The solid obtained was recrystallized from hot methanol. Colour = Shining black,Yield: 0.529 g (68%); m.p. > 300°C;Analysis Calcd. for C$_{41}$H$_{48}$Cl$_2$N$_2$O$_2$Ti$_2$(767.47): C, 64.16; H, 6.30; N 3.65; Ti 12.47.Found: C, 64.06; H, 5.20; N, 3.55; Ti, 12.37. μ_{eff} = 2.80 BM. Molar conductance Λm at 25 °C (Ω^{-1} cm^2 mol^{-1}): 56 in DMSO. Selected infrared absorption (KBr, cm^{-1}): 1621 ν(HC=N), 509 ν(M-O), 622 ν(M-N). Electronic spectra (λ_{max} in nm, ε in M^{-1}cm^{-1}) in DMF: 310 (720), 330 (1660). ESI-Mass spectra, m/z: $[C_{17}H_{16}N_2O_2 + 3H^+]^+$ = 283.12, $[C_{22}H_{27}NOTi + H^+]^+$ = 370.16, $[C_{41}H_{48}N_2O_2Ti_2 + 2H^+]^+$ = 697.27, $[C_{41}H_{48}Cl_2N_2O_2Ti_2]^+$ = 731.77, $[C_{41}H_{48}Cl_2N_2O_2Ti_2 + H]^+$ = 768.20, Mτ = 767.20.

DFT Study
The geometry of ligand and complexes was optimized by DFT method of B3LYP and/or LANL2DZ basic set manifested by Gaussian 09 (Frisch *et al.,* 2009). The quantum chemical parameters such as HOMO, LUMO energies were calculated using TD-SCF, DFT/6-311G at the B3LYP level of theory. The parameters such as Δ**E**, Mulliken electronegativity (**χ**), dipole moment, chemical potential (**μ**), global hardness (**η**), global softness (**S**), global electrophilicity (**ω**), absolute softness (**σ**) and electronic charge (Δ**N$_{max}$**) was calculated.

Biological activity
Ligands and complexes were screened for antibacterial activity against gram negative bacteria *E. coli*, (ATCC no. 35218) at different concentration. Agar well diffusion method was used for antibacterial screening as discussed earlier (Mehrotra *et. al.,* 2015).

Results and discussion

Characterization of ligands

Empirical formulae of Schiff base ligands were in agreement with elemental analysis. ESI-Mass spectra of the ligands, **L$_1$, L$_2$** and **L$_3$** exhibit several peaks depending upon the fragmentation pattern. A molecular/pseudomolecular ion peak was observed in each ligand confirming their molecular weight. The

Research Article

ESI-MS spectra of the ligand, L_1 (Fig.1) shows peaks at m/z 177.11, 218.13, 163.09, 149.07, 311.17 attributed for $[C_{11}H_{14}NO + H]^+$; $[C_{13}H_{17}N_2O + H]^+$; $[C_{10}H_{12}NO+ H^+]^+$; $[C_9H_{10}NO+ H^+]^+$ and $[C_{19}H_{22}N_2O_2 + H^+]^+$ respectively. The peak observed at m/z 311.17 was due to pseudo molecular ion. ESI-MS of L_2 exhibit peak at 163.09, 190.23 and 283.34 attributed for $[C_{10}H_{12}NO + H]^+$; $[C_{11}H_{13}N_2O + H]^+$; and $[C_{17}H_{18}N_2O_2+ H^+]^+$ respectively. A peak at 283.34 was due to pseudo molecular ion. ESI-MS of L_3 exhibit peak at 153.04, 167.05, 181.06, 208.06, 283.02 and 319.06 assigned for $[C_8H_7ClN + H]^+$, $[C_9H_9ClN + H]^+$, $[C_{10}H_{11}ClN + H]^+$, $[C_{11}H_{12}ClN_2 + H]^+$, $[C_{17}H_{16} ClN_2 + H]^+$ and $[C_{17}H_{16}Cl_2N_2 + H^+]^+$. Peak at *m/z* 318.06 was due to pseudo molecular ion. The ESI-MS spectrum of ligand L_1 is shown in Figure 1.
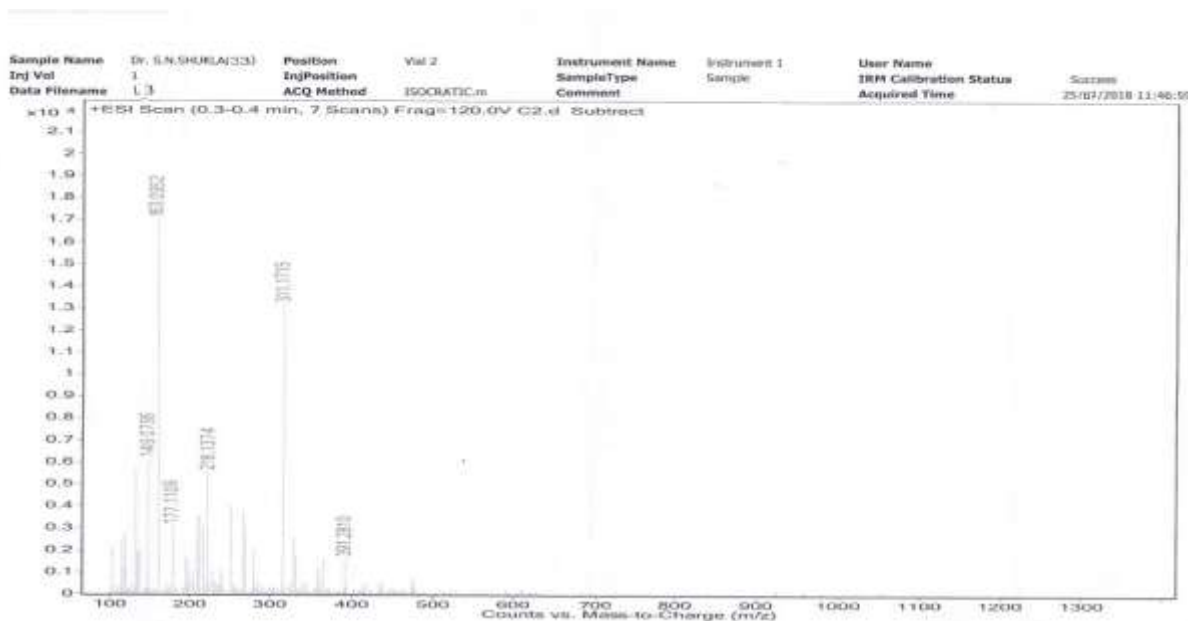

Figure 1: ESI MS spectrum of ligand L_1

FT IR spectra of ligands L_1, L_2 and L_3 display a signal at ~1615 cm^{-1} was attributed to ν(HC=N) group. Ligand L_1 and L_2 exhibit a broad/ weak signal between ~3356 cm^{-1} attributed for ν(O-H) stretching vibration (Silverstein *et. al.*, 1991). FT-IR spectra of L_1 is shown in Figure 2.

^{1}H-NMR of ligand L_1 exhibit a singlet at δ 14.348 ppm for 2H attributed for the two phenolic-OH group. It also exhibit a multiplet centered at δ 6.777 ppm for four protons, triplets centered at δ 7.279 ppm for two protons with coupling constant 18 and 20 Hz and doublet centered at δ 7.637 for two protons with coupling constant 20 Hz attributed to aromatic ring protons. A multiplet centered at δ 3.686 ppm for 6H was assigned for methylene protons. A singlet at δ 2.044 ppm for 6H was attributed for methyl the two methyl group. Proton NMR spectra of L_1 is displayed in Figure 3.

^{1}H-NMR of L_2 exhibit a singlet at δ 12.154 ppm for 2H assigned for phenolic-OH. It also exhibit two triplets centered at δ 6.648 ppm and δ 7.185 ppm for two proton each and two doublets centered at δ 7486 ppm and δ 7.506 ppm for two proton each was attributed for aromatic proton. A multiplet centered at δ 3.634 ppm for six protons was assigned for methylene group.

^{1}H-NMR of L_3 exhibit a singlet centered at δ 8.456 ppm for two proton assigned for (-HC=N)$_{imine}$ group. Two doublets centered at δ 6.948 ppm and δ 7.028 ppm for 4H each were attributed for aromatic ring present. A multiplet centerd at δ 3.302 ppm for 6H was assigned to methylene group.
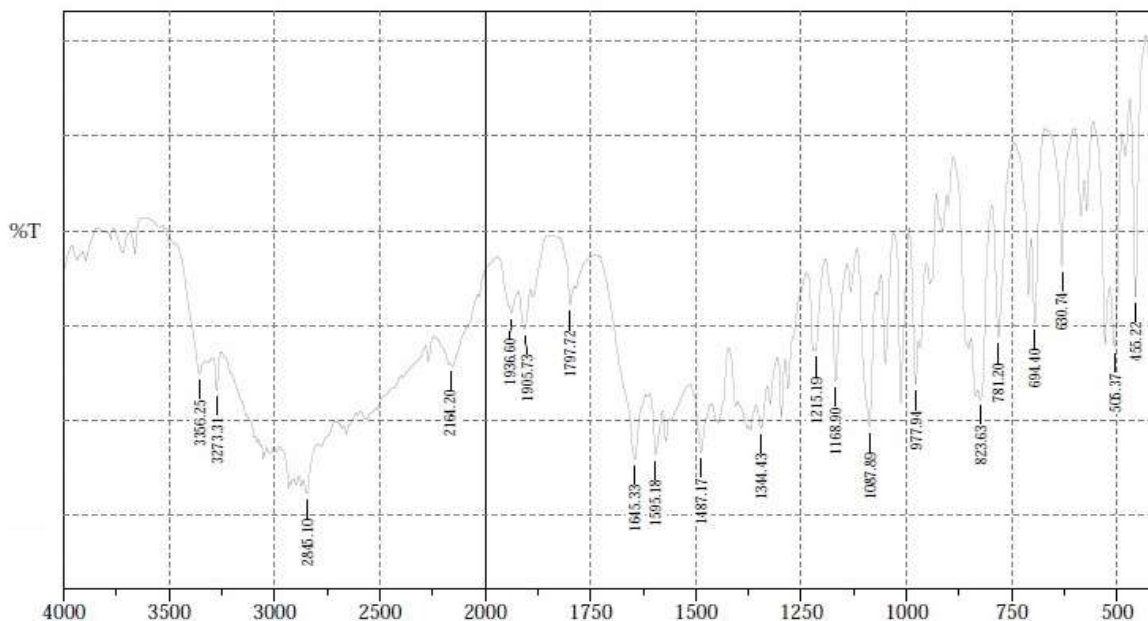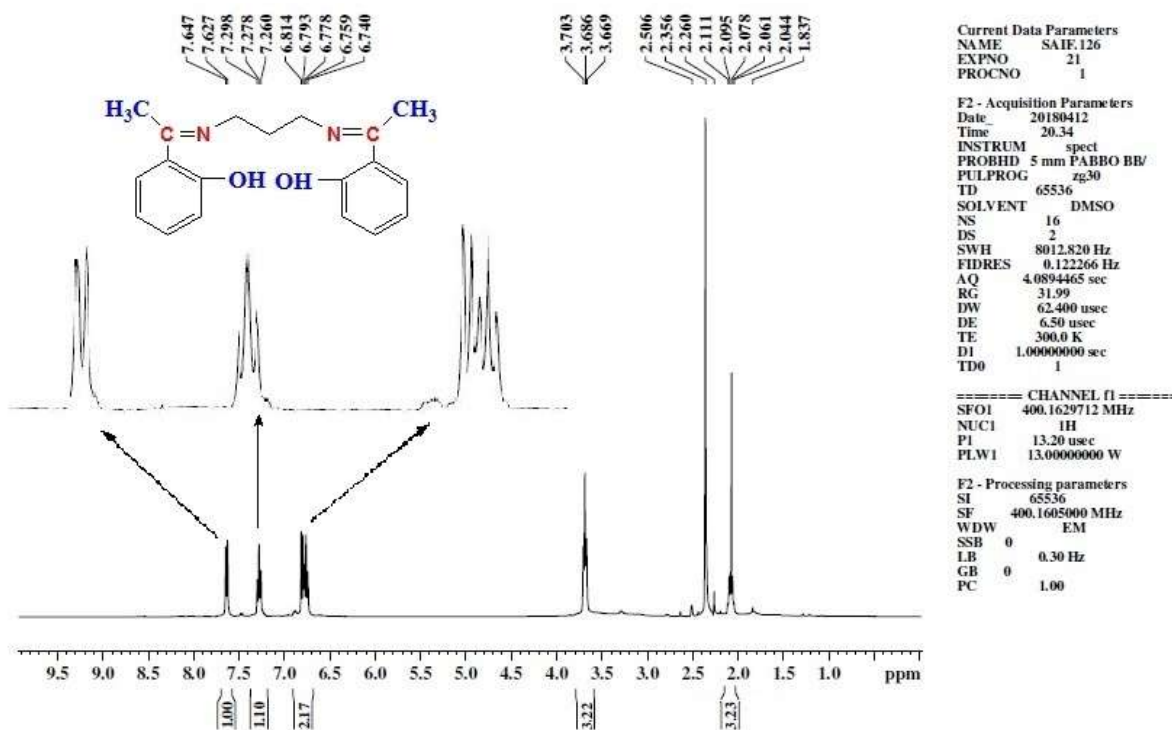
Figure 2: FTIR Spectrum of ligand L1

Figure 3: ¹H-NMR Spectrum of L1

Research Article

^{13}C-NMR of **L$_1$** exhibit signal at δ 163.80 ppm assigned for azomethine δ(>C=N)$_{imine}$ carbon. Signal at δ 172.82 ppm was attributed for aromatic carbon linked with hydroxyl group. However, other aromatic carbons have displayed signal between δ 116.48 – 132.35 ppm. The signals at δ 46.13 ppm and δ 14.28 ppm were attributed for methyle and methyl carbon respectively. ^{13}C-NMR of **L$_2$** exhibit signal at δ 162.84 ppm assigned for azomethine δ(>C=N)$_{imine}$ carbon. Signal at δ 170.89 ppm was attributed for aromatic carbon linked with hydroxyl group. However, other aromatic carbons have displayed signal between 116.52-148.58 ppm. The signals at δ 43.06 ppm was attributed for methylene carbon.

^{13}C- NMR of **L$_3$** exhibit signals at δ 162.84 ppm was assigned for δ(-CH=N) $_{imine}$ carbon. The signal between δ 115.50-140.38 ppm were attributed to aromatic carbon. The signal at δ 44.92 ppm was assigned for methylene carbon. ^{13}C- NMR spectra of ligand **L$_1$** is shown in Figure 4.Thus on the basis of elemental analysis, ESI MS, FT-IR, ^{1}H-NMR and ^{13}C-NMR following structure (Figure 6) of ligands were suggested.
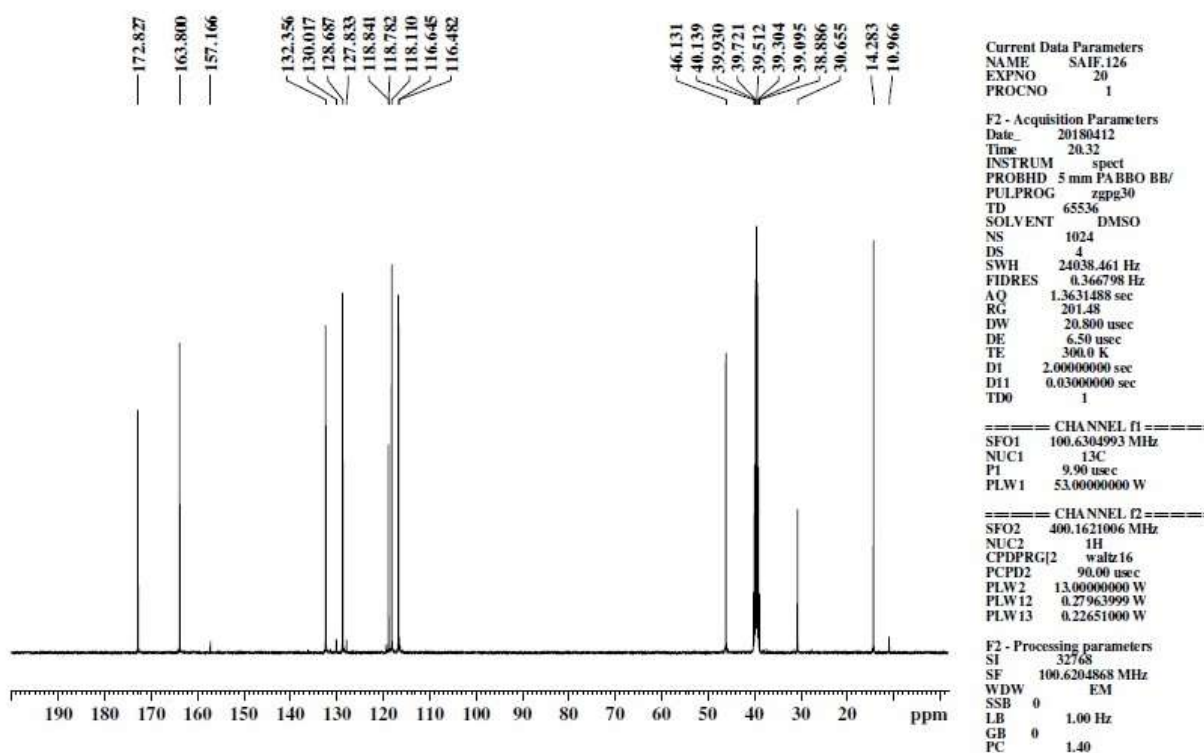

Figure 4: ^{13}C- NMR Spectrum of L$_1$

UV–Vis spectra of ligands exhibit two absorption bands at ~240 nm and ~300 nm. The first band of low extinction was assigned to π→ π* transition associated with the aromatic ring. Another band of high intensity at ~300 nm, was attributed to n→ π*transition for (>C=N) imine nitrogen. Electronic spectra of ligand **L$_1$** is given in Figure 5.
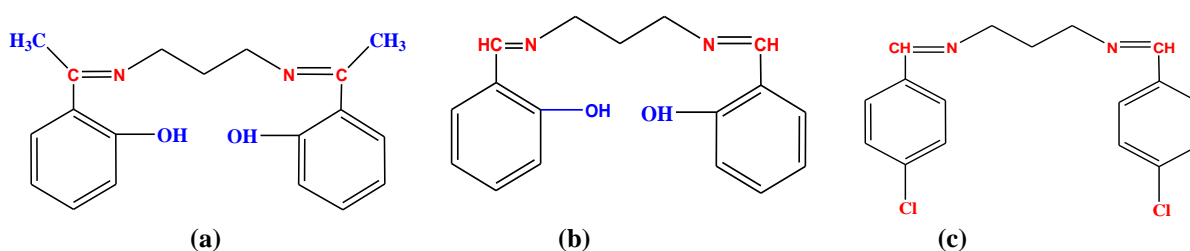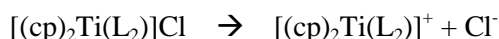
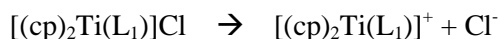**Research Article**
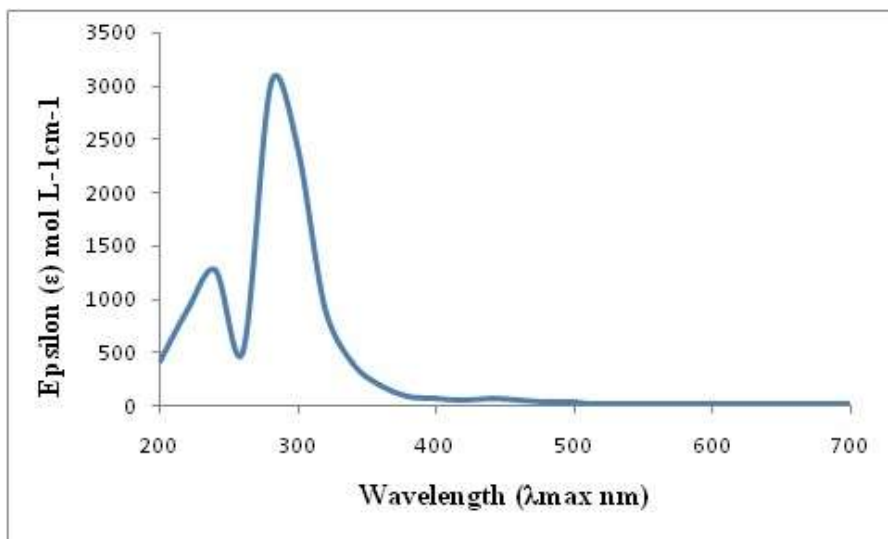
Figure 5: UV-Vis spectrum of L₁

(a)   **(b)**   **(c)**

Figure 6: Structure of ligands (a) L_1, (b) L_2 and (c) L_3.

Characterization of complexes

Stoichiometries of complexes were in agreement with elemental analysis. Molecular conductance of complexes **1** and **2** was in between 28 - 30 S cm^2 mol^{-1} indicating the 1: 1 electrolytic nature. However, complexes **3, 4** and **5** exhibit molar conductance in between 56 - 68 S cm^2 mol^{-1}, indicating 1: 2 nature of complexes (Geary, 1971). The presence of Cl$^-$ ion outside the coordination sphere was tested qualitatively by silver nitrate test.

ESI-MS of complexes exhibit several molecular ion and pseudomolecular ion peak indicating their molecular weight. ESI-MS of complex **1** exhibit peak at m/z 177.11, 311.16, 342.12, 517.50 and 553.90. The peak at m/z m/z 177.11, 311.16 and 342.12 were assigned for $[C_{11}H_{14}NO + H]^+$, $[C_{19}H_{21}N_2O_2 + 2H]^+$ and $[C_{20}H_{23}NOTi + H]^+$. However, peak at m/z 553.90 was attributed to pseudomolecular $[M + H]^+$ and another peak at m/z 517.50 was attributed to molecular ion, M$^+$ ion formed due to ionization of Cl$^-$. In complex **2** peaks were observed at m/z 163.09, 282.13, 328.11, 489.20 and 525.17. The peak at m/z 163.09, 282.13 and 328.11 were assigned for fragments $[C_{10}H_{12}NO + H]^+$, $[C_{17}H_{17}N_2O_2 + H]^+$ and $[C_{19}H_{27}NOTi + H]^+$. However, the peak at m/z 525.17 was ascribed to pseudomolecular ion $[M + H^+]^+$ and another peak at m/z 489.20 was attributed to M$^+$ formed due to ionization of Cl$^-$. From ESI-MS and molar conductance data, it was confirmed that in both case complexes are 1:1 electrolyte and ionize to produce two ions as follows:

$$[(cp)_2Ti(L_1)]Cl \rightarrow [(cp)_2Ti(L_1)]^+ + Cl^-$$

$$[(cp)_2Ti(L_2)]Cl \rightarrow [(cp)_2Ti(L_2)]^+ + Cl^-$$

Research Article

In complex **3** ESI-MS peaks were observed at m/z 319.06, 561.56 and 598.06. The peak at m/z 319.06 was ascribed to $[L + H^+]^+$. However, peak at m/z 561.56 was attributed to $[M + Cl^-]^+$ and another peak at m/z 598.06 was assigned for pseudomolecular ion $[C_{29}H_{31}Cl_4N_2Ti + H]^+$. ESI-MS of complex **4** exhibit signal at m/z 311.15, 384.17, 725.53, 760.17 and 796.53 assigned for $[C_{19}H_{20}N_2O_2 + 3H^+]^+$, $[C_{23}H_{29}NOTi + H^+]^+$, $[C_{43}H_{52}N_2O_2Ti_2 + H^+]^+$, $[C_{43}H_{52}ClN_2O_2Ti_2]^+$ and $[C_{43}H_{52}Cl_2N_2O_2Ti_2 +H]^+$. The peak at m/z 796.53 was attributed to pseudomolecular $[C_{43}H_{52}Cl_2N_2O_2Ti_2 +H]^+$. ESI-MS of complex 5 exhibit peak at m/z 283.12, 370.16, 697.27, 731.77 and 768.20 assigned for $[C_{17}H_{16}N_2O_2 + 3H^+]^+$, $[C_{22}H_{27}NOTi + H^+]^+$, $[C_{41}H_{48}N_2O_2Ti_2 + 2H^+]^+$, $[C_{41}H_{48}Cl_2N_2O_2Ti_2]^+$ and $[C_{41}H_{48}Cl_2N_2O_2Ti_2 + H]^+$. The peak at 768.20 was ascribed to pseudomolecular ion $[C_{41}H_{48}Cl_2N_2O_2Ti_2 + H]^+$. ESI-MS of complex 1 was shown in Figure 7.
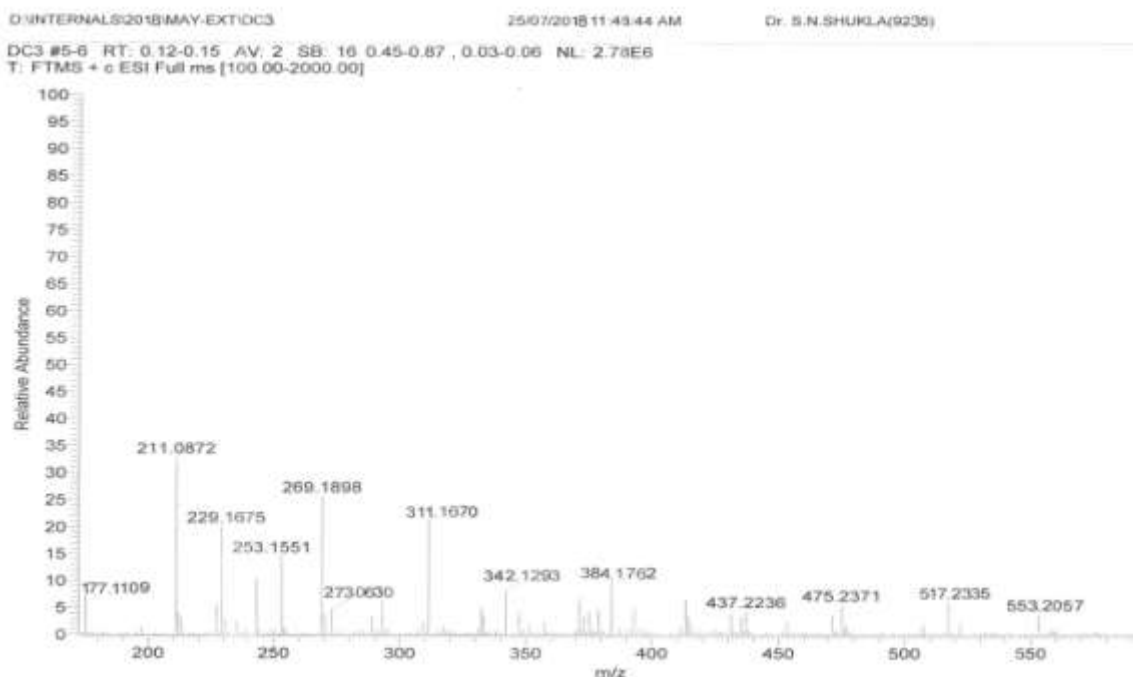

Figure 7: ESI-MS spectrum of complex 1

In FT-IR spectra, the peak observed at ~1620 cm^{-1} in Schiff base ligands for (>C=N) was shifted to lower wave number and appeared at ~1604 cm^{-1} indicating coordination of metal through imine-N. It was also confirmed by appearance of a peak at ~490 cm^{-1} attributed to ν(M-N) stretching (Sujamol *et. al.,* 2010). However, in complex **1** and **2** a shoulder observed at ~1624 cm^{-1} was indicative of presence of one uncoordinated >C=N group along with coordinated >C=N. The peak appeared at ~3327 cm^{-1} in ligands **L₁** and **L₂** assigned for ν(O-H) was shifted to lower wave number in complex **1** and **2.** However, it vanished completely in the complexes **4** and **5** and a weak band appeared at ~510 cm^{-1} was ascribed to formation of M-O bond in complexes by removal of phenolic-H. FT-IR spectrum of complex **1** was displayed in Figure 8.

Since all complexes were paramagnetic, NMR spectra of the complexes were complicated. In diamagnetic molecules the orbital shift (*dorb*) provides the principal contribution to the observed chemical shifts. In paramagnetic samples the hyperfine shift (*d$_{hf}$*) adds to the orbital shift, leading to major change in the observed chemical shift:
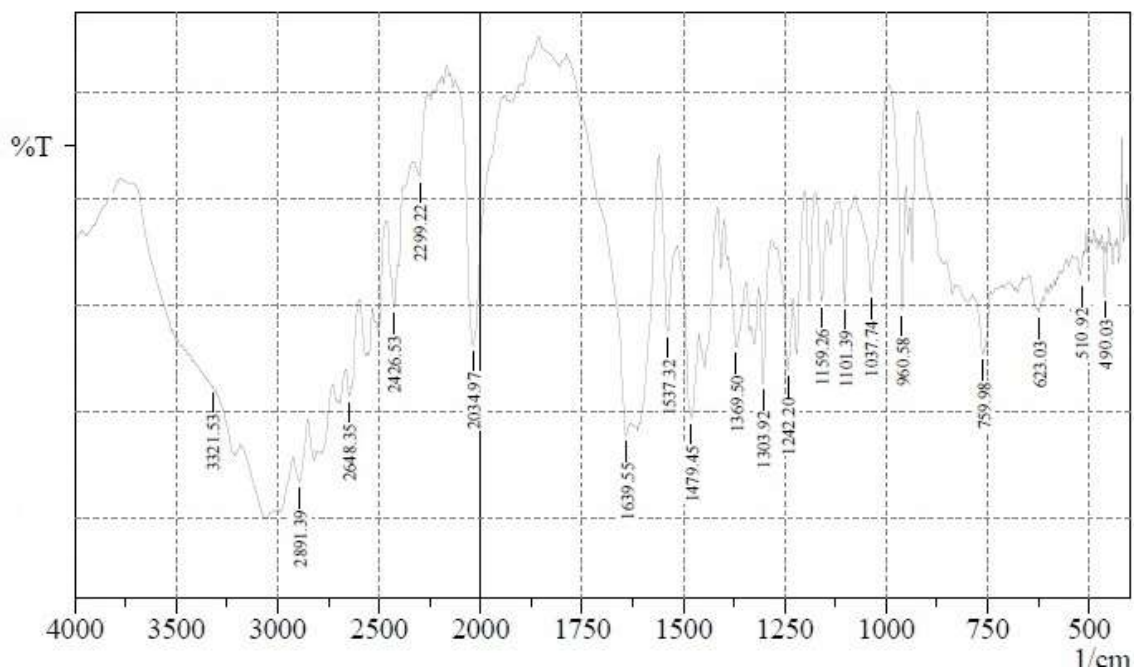
$$d_{obs} = d_{orb} + d_{hf}$$

Research Article
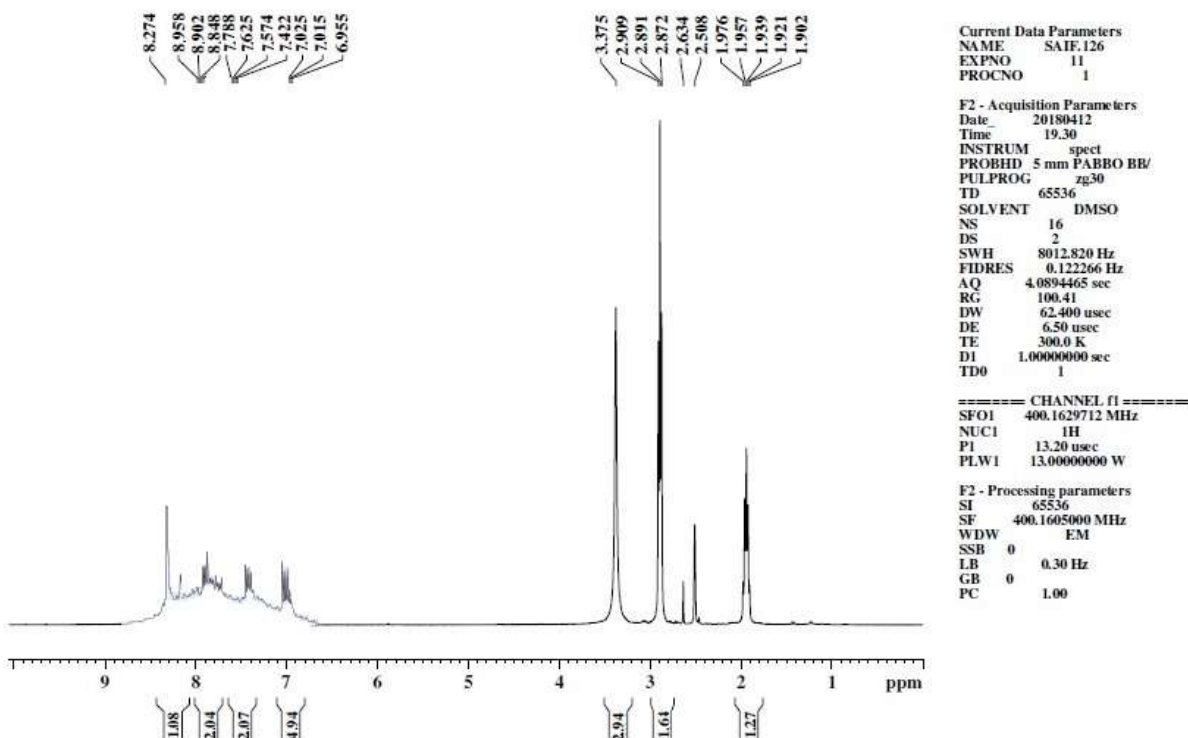

Figure 8: FT-IR spectrum of complex 1

Figure 9: ^{1}H-NMR Spectrum of complex 1

Research Article

In view of common evidences and inevitable paramagnetic interference, we have explained ^{1}H-NMR spectra of complex **1**. Observation of signal in aromatic region reveals the presence of the calculated number of aromatic protons. In aromatic reagion four set of signals were observed. A broad multiplet appeared between δ 6.955- δ 7.020 ppm was attributed for 10 protons of two cyclopentadienyl ring of titanocene moiety. Another broad multiplet centered at ~δ 7.625 ppm for four protons was atributed for aromatic proton associated with uncoordinated phenolic ring. However, broad multiplet centered at ~ δ 8.902 ppm was assigned for four proton of coordinated phenolic ring. This is also an evidence for coordination of only one imine group in the complexes. The signal appeared at δ 3.375 ppm was attributed for six methylene proton. A signal centered at ~ δ 2.891 ppm for three protons was assigned for methyl proton associated with coordinated imine moiety. However, a signal centered at δ 1.921 ppm for three proton was attributed for methyl proton associated with uncoordinated imine moiety. .The ^{1}H-NMR spectrum of complex **1** is shown in Figure **9.**

^{13}C-NMR spectrum of complex **1** (Figure 10) exhibit several signals in between δ 24.98 – δ 173.17 ppm. Signal between δ 117.54 – δ 119.13 ppm were attributed to cyclopentadienyl carbon. However, singlets observed between δ 131.35 ppm – δ 136.37 ppm were attributed to different carbon of the phenolic ring. The two signals observed at δ 165.57 ppm and δ 162.68 were attributed for the presence of two nonequivalent azomethine carbon. The signal observed at higher δ value was attributed to the azomethine carbon coordinated to titanium metal and another signal was assigned for the uncoordinated azomethine carbon. The two signal observed at δ 173.17 ppm and δ 172.88 ppm were attributed to the presence of two non equivalent aromatic carbon linked with hydroxyl moiety in which one is coordinated and other is uncoordinated.
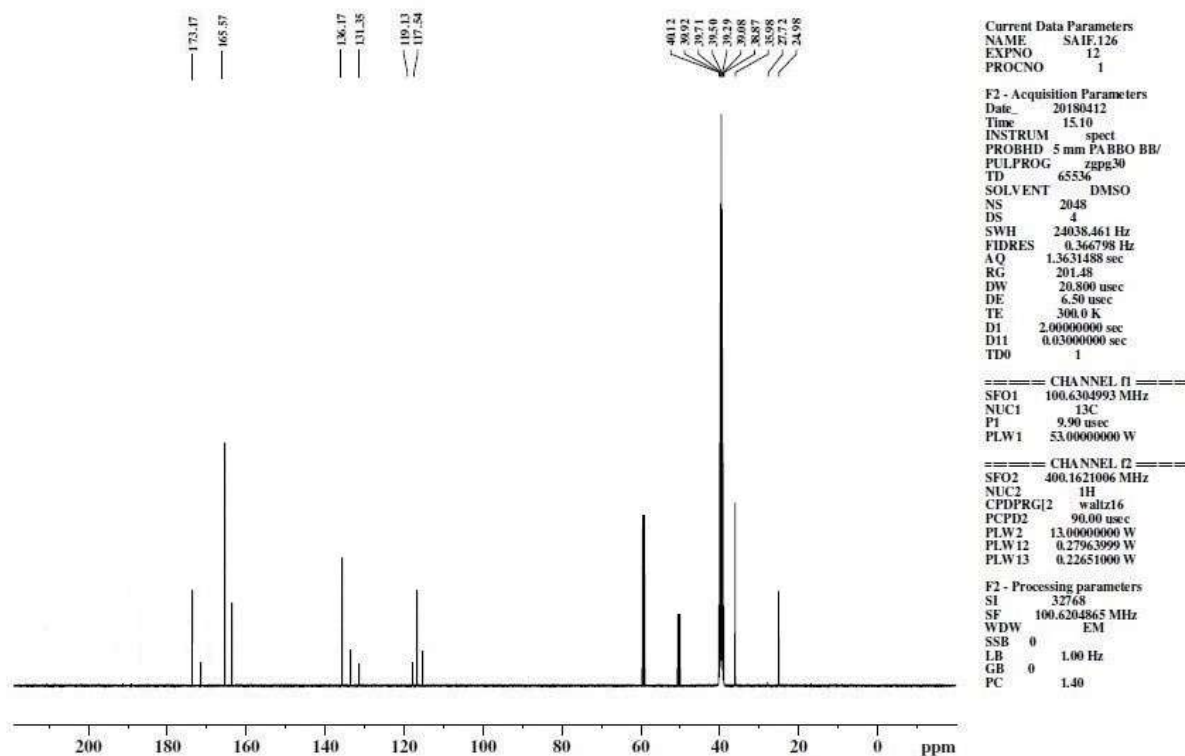
Figure 10: ^{13}C-NMR spectrum of complex 1

The electronic spectra of complexes exhibit three bands in UV-Visible range. The two bands, observed in ligands attributed to π→ π* and n→ π* were bathochromic shifted and appeared at ~ 300 nm and at ~ 340

Research Article

nm, Shifting of n→ π* band to higher wavelength clearly indicates the transfer of electron pair from azomethine-N to metal (Lever 1984), (Aswar and Badwaik, 2007). The bands at ~ 480 nm was attributed to d-d transition of Ti(II) ion.The electronic spectrum of complex **1** is given in Figure 11.
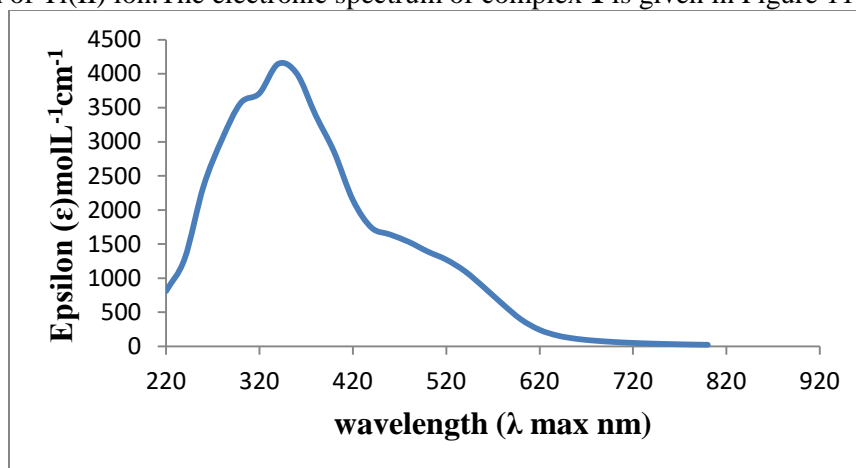
Figure 11: UV-Vis spectrum of complex 1

Thus on the basis of elemental analysis, molar conductance, ESI MS, FT-IR, ^{1}H-NMR and ^{13}C-NMR following structure of complexes were suggested (Figure 12).

(a)   **(b)**   **(c)**

(d)   **(e)**

Figure 12 : Structure of (a) complex 1, (b) complex 2, (c) complex 3, (e) complex 4, (d) complex 5

Bond parameters

Research Article

Determination of the molecular structure of complexes in the absence of single crystal was done by DFT optimizations in the gas phase of ligands and complexes. The optimized bond lengths, bond angle and dihedral angles of investigated compound were calculated by B3LYP methods with 6-31++G (d, p) basis set were listed in Table 1 and 2 in accordance with atom numbering scheme as shown in Figure 14(a), (b), (c)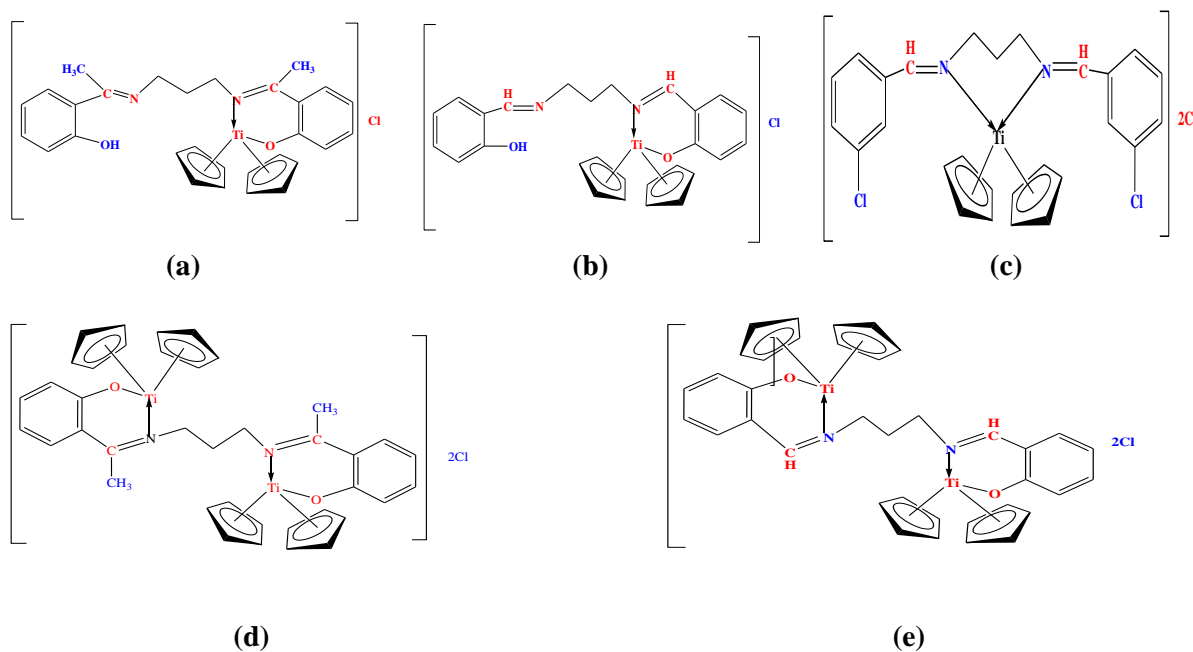, (d) and (e). The optimized geometrical parameters of ligands are compared with complexes. Bond length of azomethine >C=N in ligands was ~ 1.29 Å, which increases in the case of complex **1**, **2** and **3** and observed as ~ 1.30Å. This increase in bond distance was because of transfer of electron density of double bond towards metal and decrease in the double bond character of >C=N, which in turn confirms the coordination of metal with azomethine-N. The calculated C-O bond distances in ligand **L₁** and **L₂** was ~ 1.43 Å, which was slightly shorter than free ligands and observed as ~ 1.42 Å in complex **1** and **2**. However, in complex **3** and **4,** C-O bond distances were slightly higher. The optimized structure for the ligands and complexes were proposed in Figure 14(a), (b), (c), (d), and (e).

Table 1: Selected geometrical parameters of Ligands and Complexes

S. No.	Ligand / Complex		E_{HOMO} (eV)	E_{LUMO} (eV)	ΔE (eV)	χ (eV)	η (eV)	σ (eV⁻¹)	Pi (eV)	S (eV⁻¹)	ω (eV)	$ΔN_{max}$ (eV)	Total energy (a.u.)	Diple moment (Debye)
1	Ligand 1		-3.941	-2.113	1.828	3.027	0.914	1.094	-3.027	0.547	5.014	3.312	-996.178	3.2667
2	Ligand 2		-4.797	-2.728	2.068	3.762	1.034	0.966	-3.762	0.483	6.843	3.637	-917.909	5.6142
3	Ligand 3		-4.822	-2.534	2.288	3.678	1.144	0.874	-3.678	0.437	5.914	3.215	-1686.545	3.1423
4	Complex 1	A	-3.279	-2.02	1.259	2.649	0.629	1.588	-2.649	0.794	5.575	4.208	-1441.320	8.1047
		B	-3.171	-2.030	1.143	2.600	0.570	1.752	-2.600	0.876	5.926	4.557		
5	Complex 2	A	-3.430	-1.992	1.437	2.711	0.718	1.391	-2.711	0.695	5.114	3.772	-1363.098	7.6739
		B	-3.291	-1980	1.311	2.635	0.655	1.524	-2.635	0.762	5.297	4.019		

Table 2: The calculated quantum chemical parameters of ligands and complexes

Bond Connectivity Bond Length (in Angstrom Å)							
(Ligand 1)	(Ligand 2)	(Ligand 3)	Complex 1	Complex 2	Complex 3	Complex 4	Complex 5
(C2-N19) 1.46798	(C1-N10) 1.46998	(C1-N12) 1.47000	(C1-N4) 1.46832	(C1-N4) 1.46832	(C1-N4) 1.46781	(C2-N5) 1.50343	(C3-N4) 1.51527
(C3-N20) 1.46786	(C3-N11) 1.46997	(C3-N13) 1.47000	(C3-N5) 1.47320	(C3-N5) 1.47320	(C3-N5) 1.49667	(C3-N4) 1.51527	(C2-N5) 1.50343
(H34-O32) 0.96325	(H38-O36) 0.95998	-	-	-	-	-	-
(H35-O33) 0.95972	(H39-O37) 0.96001	-	-	-	-	-	-
AZOMETHINE (C4=N19) 1.29331	AZOMETHINE (C13=N10) 1.29361	AZOMETHINE (C4=N12) 1.29360	AZOMETHINE (C6=N4) 1.3033	AZOMETHINE (C6=N4) 1.3035	AZOMETHINE (C6=N4) 1.3369	AZOMETHINE (C6=N4) 1.27427	AZOMETHINE (C6=N4) 1.27427
(C6=N20) 1.29401	(C12=N11) 1.29360	(C11=N13) 1.29360	(C7=N5) 1.33359	(C7=N5) 1.33359	(C7=N5) 1.33814	(C7=N5) 1.35943	(C7=N5) 1.35943
(C4-C5) 1.54518	(C13-H14) 1.07002	(C4-H15) 1.07000	(C6-C9) 1.54230	(C6-C17) 1.54577	(C6-C18) 1.53980	(C6-C83) 1.54000	(C6-C11) 1.45107
(C6-C7) 1.53987	(C12-H15) 1.07000	(C11-H14) 1.07000	(C7-C8) 1.53862	(C7-C28) 1.57232	(C7-C29) 1.54005	(C7-C82) 1.54000	(C7-C22) 1.60597
-	-	-	-	-	-	(C6-C11) 1.45107	-

Research Article

						(C7-C22) 1.60597	-
-	-	-	-	-	-	(C7-C22) 1.60597	-
(C23-O32) 1.43073	(C18-O36) 1.43000	-	(C24-O42) 1.4286	(C16-O34) 1.4287	-	(C10-O28) 1.5424	(C10-O28) 1.5423
(C36-O33) 1.42968	(C31-O37) 1.43005	-	(C37-O43) 1.44204	(C29-O35) 1.44204	-	(C23-O29) 1.44294	(C23-O29) 1.44294
-	-	(C17-Cl35) 1.76000	-	-	-	-	-
-	-	(C25-Cl34) 1.76000	-	-	-	-	-
-	-	-	-	(C6-H60) 1.13085	(C6-H14) 1.07000	-	(C6-H83) 1.07000
-	-	-	-	(C7-H61) 1.28856	(C7-H15) 1.07017	-	(C7-H82) 1.07000
-	-	-	(O43-Ti45) 1.94823	(O35-Ti37) 1.9482	-	(O28-Ti36) 1.91451	(O28-Ti36) 1.91451
-	-	-	-	-	-	(O29-Ti37) 1.93978	(O29-Ti37) 1.93978
-	-	-	(N5-Ti45) 1.98834	(N5-Ti37) 1.98834	(N4-Ti36) 1.95719	(N4-Ti36) 2.11328	(N4-Ti36) 2.11328
-	-	-	-	-	(N5-Ti36) 1.97849	(N5-Ti37) 1.95088	(N5-Ti37) 1.95088
-	-	-	-	-	(C16-Cl48) 1.75964	-	-
-	-	-	-	-	(C27-Cl49) 1.75987	-	-
-	-	-	(Ti45-C46) 2.08806	(Ti37-C38) 2.0880	(Ti36-C37) 2.09014	(Ti36-C60) 2.12157	(Ti36-C60) 2.12157
-	-	-	(Ti45-C57) 2.09192	(Ti37-C49) 2.0919	(Ti36-C37) 2.09004	(Ti36-C71) 2.07993	(Ti36-C71) 2.07993
-	-	-	-	-	-	(Ti37-C38) 2.06570	(Ti37-C38) 2.06570
-	-	-	-	-	-	(Ti37-C49) 2.07914	(Ti37-C49) 2.07914

Molecular electrostatic potential analysis (MEP) and contour maps
A well-remarked molecular electrostatic surface potential (MESP) charge regionalization is set up with the help of electron density plot. In that, nucleophilic centers (negative regions), electrophilic sites (positive regions) are pointed out. The potential surface diagrams of ligand and its complex as shown in Figure 13. MEP of Ligand L_1 and complex **1** indicates that the hydroxyl oxygen and azomethine-N atoms represent the negative potential region. The hydrogen atoms bear the region of maximum positive charge.

-9.334e-2 ▬▬▬▬▬ +9.334e-2   -8.183e-2 ▬▬▬▬▬ +8.183e-2

Figure 13. (a) Molecular Electrostatic Potential (MEP) of Ligand L_1 and complex C_1
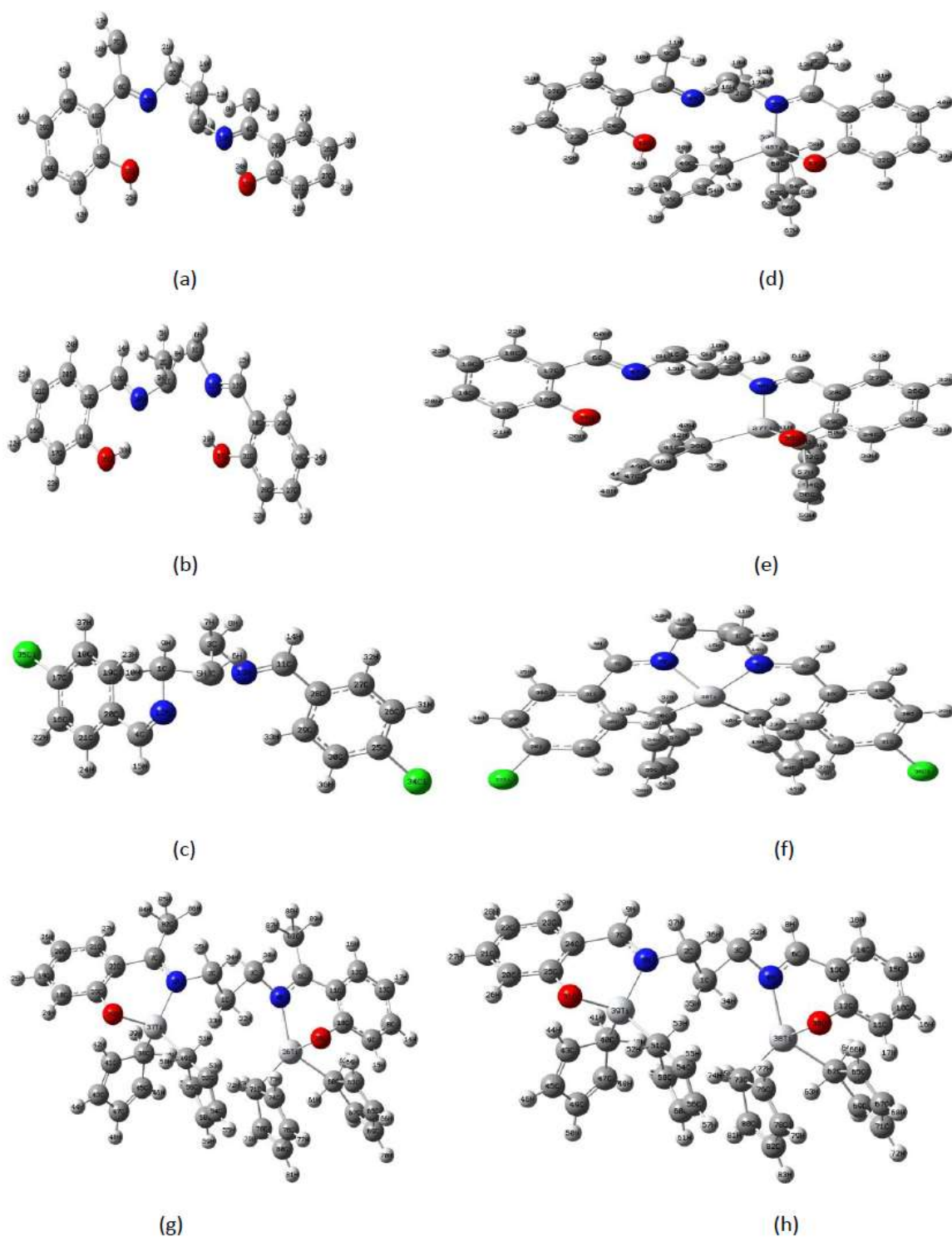
Research Article

Figure 14: DFT optimized structure of (a) Ligand L₁ (b) Ligand L₂ (c) Ligand L₃ (d) complex 1 (e) complex 2 (f) complex 3 (g) complex 4 (h) complex 5

Research Article

Mulliken atomic charge analysis

Mulliken atomic charge computation (Mulliken 1955) and natural charge population analyses (Redd *et. al*., 1985) of natural bond orbital (NBO) have a remarkable part in the use of quantum chemical estimation to the molecular framework on account of atomic charges impact, electronic structure, molecular polarizability, dipole moment and other properties of the framework. The comparative values of both scales for L_1 and complex **1** are represented in the O and N atoms exhibit a negative charge because of their donating property. Hydrogen atoms of L_1 and metal atom of complex **1** displayed positive charges because of their accepting property. Therefore, Mulliken populations and natural populations appear as a complementary tool to the molecular electrostatic potential *(*MEP) approximation for studying reactivity, and the correlation between results obtained from each scheme. Charge distribution on each atom of L_1 and complex 1 is shown in **Figure 15 (a-d)** and also as bar diagrams in **Figure15-16 (a)** and **(b)**.
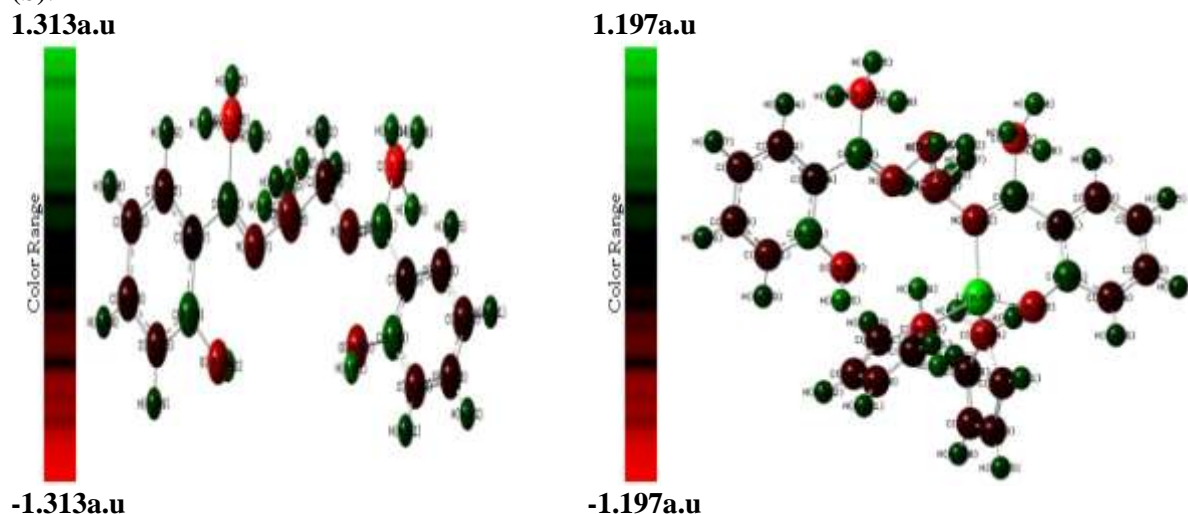

Figure 15 (a) Natural atomic charges of ligand L_1, **(b) Natural atomic charges of complex**
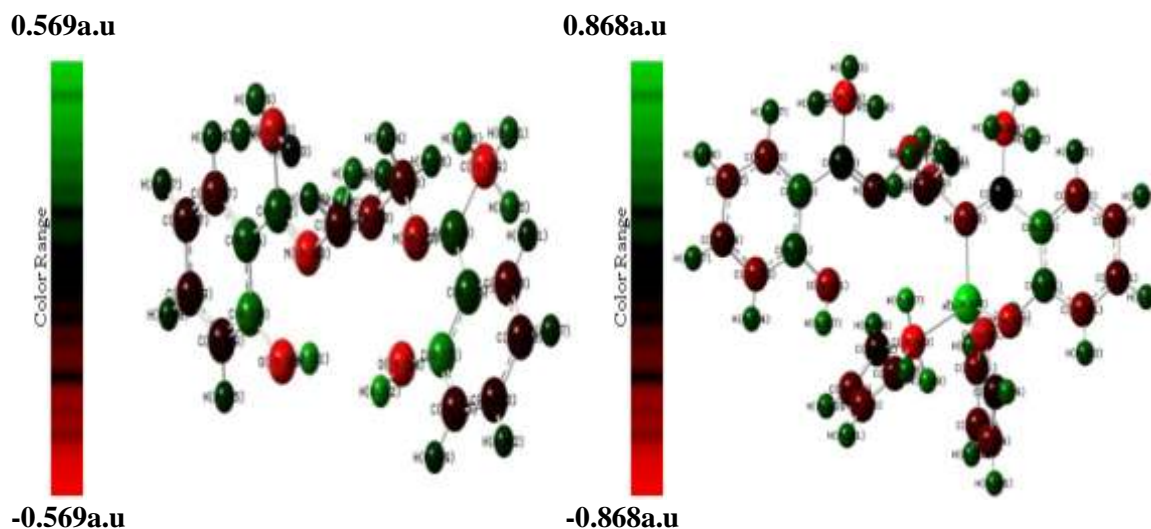

Figure 16: (d)Mulliken atomic charges of ligand L_1 (e) Mulliken atomic charges of complex 1

Catalytic activity of complexes in Ring - opening polymerization (ROP) reaction of ε-caprolacton

Research Article

Polymerization reaction was carried out with different amount of catalyst (2.60×10^{-2} - 3.81×10^{-2} mmol) at 125 °C, for different reaction time such as 6 h, 12 h and 24 h using complex **1**-**5** as catalyst. The results obtained for PCL synthesis at different conditions are given in Table 3, it could be observed from the table that maximum yield of PCL was obtained when complex **5** was used as catalyst. The optimum condition for this yield of 73.4 % was 125 °C, 24 h and 0.020 g. The outstanding performance of complex **5** could attributed to the presence of two metal center in the molecules. However, complex **3** exhibit lower performance probably due to absence of M-O bond, which actually assumed to start the reaction by insertion of ε-capralactone.

Table 3: Optimization of reaction conditions for PCL synthesis

Complexes	ε-caprolactone		Complexes		Temperature	Time	Yield		Mn-Value
	mL	Mmol	Gram	Mmol	°C	hour	mg	%	
Complex 1	0.97	8.8	0.020	3.61×10^{-2}	125ºC	6	0.236	23.6	43347
	0.97	8.8	0.020	3.61×10^{-2}	125ºC	12	0.259	25.9	54370
	0.97	8.8	0.020	3.61×10^{-2}	125ºC	24	0.271	27.1	62872
Complex 2	0.97	8.8	0.020	3.81×10^{-2}	125ºC	6	0.388	38.8	48626
	0.97	8.8	0.020	3.81×10^{-2}	125ºC	12	0.397	39.7	60919
	0.97	8.8	0.020	3.81×10^{-2}	125ºC	24	0.415	41.5	81637
Complex 3	0.97	8.8	0.020	3.34×10^{-2}	125ºC	6	0.184	18.4	38515
	0.97	8.8	0.020	3.34×10^{-2}	125ºC	12	0.199	19.9	46799
	0.97	8.8	0.020	3.34×10^{-2}	125ºC	24	0.224	22.4	55633
Complex 4	0.97	8.8	0.020	2.51×10^{-2}	125ºC	6	0.439	43.9	170481
	0.97	8.8	0.020	2.51×10^{-2}	125ºC	12	0.558	55.8	194671
	0.97	8.8	0.020	2.51×10^{-2}	125ºC	24	0.584	58.4	216068
Complex 5	0.97	8.8	0.020	2.60×10^{-2}	125ºC	6	0.626	62.6	177886
	0.97	8.8	0.020	2.60×10^{-2}	125ºC	12	0.689	68.9	235959
	0.97	8.8	0.020	2.60×10^{-2}	125ºC	24	0.734	73.4	277268

Anticorrosion Activity

Weight loss measurement:-

Corrosion inhibition study of ligands and their complexes were performed by using weight loss measurement method. The concentration of the ligands and their complexes was chosen to be 100 ppm each. Interestingly, it was observed from the results, that complexes have revealed better corrosion inhibition efficiency than ligands. It means complexation of Schiff base with titanium metal leads to formation of better anticorrosion agents. Moreover, complex **5** exhibits better corrosion inhibition efficiency than other complexes. The increase in corrosion inhibition efficiency of complexes was probably due to better adsorption and formation of titanium complex layer over corroding surface which inhibits the interaction of corroding surface with air O_2. Parameters namely, corrosion rate (CR) and corrosion inhibition efficiency (η %) were calculated. Results and comparative data of all the compounds are presented in Figure 17. Corrosion inhibition efficiency of compounds under investigation follows the order: Complex **5** > Complex **4** > Complex **2** > Complex **1** > Complex **3** > L**1** > L**3** > L**2**
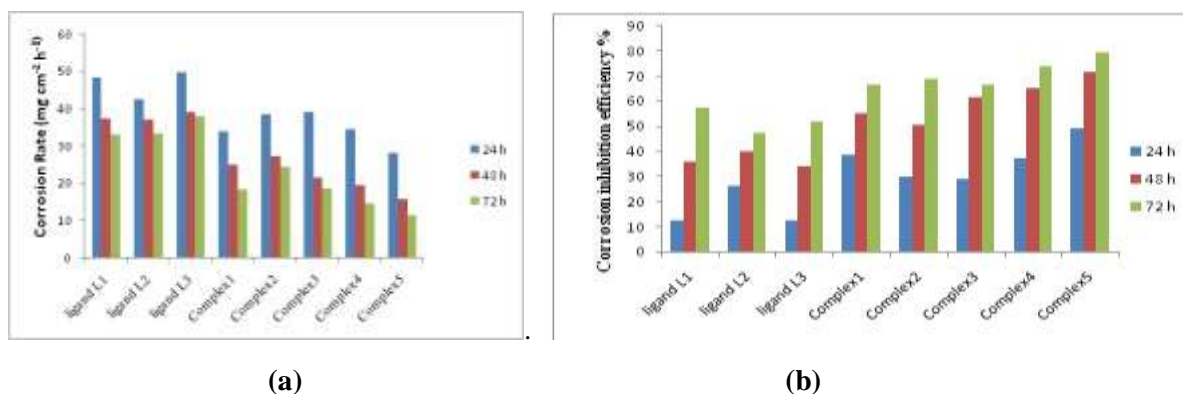
Research Article

| (a) | (b) |

Figure 17: (a) Corrosion rate of compounds, (b) Corrosion inhibition efficiency of compounds

Biological activity

Antibacterial activity

The *in vitro* antibacterial activity of the ligands and complex **1-5** were tested using the agar well diffusion method. The growth inhibition zone was measured in diameter (mm) and the results are listed in Table 5. Standard antibacterial drug amoxicillin was used as references to estimate the effectiveness of the tested compounds under the same conditions. The obtained results indicate that the complexes were more effective against *E. coli* under identical experimental conditions. It was observed that all complexes were more effective than Schiff base ligands. It was probably due to the established reason that chelation of Schiff base with metal ion enhances the lipophilicity of the central metal atom, which subsequently favours its permeation through the lipid layers of the cell membrane and blocking the metal binding sites on enzymes of microorganisms. Complex **4** has manifested higher antibacterial activity almost equal to standard drug amoxicillin. The antibacterial activity of the ligands and their complexes are found in order: **4 > 5 > 1 > 2 > 3 > L₁ > L₂ > L₃.**

Table 5: Antibacterial Screening Against *Escherichia coli*

S. No.	Ligands/ Complexes	Activity against *E. coli*	*Diameter of inhibition zone (in mm.)
1	Standard: amoxicillin	+	41
2	Schiff base ligand 1	+	29+1.5
3	Schiff base ligand 2	+	28+1.7
4	Schiff base ligand 3	+	26+0.5
5	Complex-**1**	+	36+0.8
6	Complex-**2**	+	34+0.6
7	Complex-**3**	+	32+0.2
8	Complex-**4**	+	40+1.5
9	Complex-**5**	+	39+0.6

Conclusion

Three Schiff base ligands and their five metal derivatives of titanocene dichloride have been synthesized and characterized by spectroscopic techniques. The geometries of complexes have been optimized by DFT and TD-DFT calculations. The synthesized compounds were tested for catalytic activity in the synthesis of biodegradable polymer polycaprolactone from ε-caprolactone by ring-opening polymerization. Antibacterial activity of ligands and complexes indicate that activity of ligand become more pronounced when coordinated with the metal ions. Hence, from all these extensive studies, it is

Research Article

concluded that some of these complexes could be exploited for the design of novel antibacterial drug as well as catalytic activity for polymerization of ε-caprolactone.

REFERENCES
Azam M, AlResayes SI, Wabaidur SM, Altaf M, Chaurasia B, Alam M, Shukla SN, Gaur P, Talmas N, Albaqami M, Islam MS and Park S (**2018**). Synthesis structural characterization and antimicrobial activity of Cu(II) and Fe(III) complexes incorporating azo-azomethine ligand *Molecules* **23** (1) 813.

Aswa AS and Badwaik VB (2007). Synthesis, characterization, and biological studies of some Schiff base complexes **33** 755–760.

Bhattacharjee M and Patra BN (2004). [Cp$_2$TiCl$_2$] as polymerization catalyst in aqueous medium polymerization of styrene in water *Journal of Organometallic Chemistry* **689** 1091–1094.

Erben M, Cisarova I, Honzicek J, Vinklarek J (2009). Titanocene complexes with nonlinear pseudohalide ligands: Synthesis, spectroscopic characterization and crystal structure *Inorg. Chim. Acta* **362** 2480–2486.

Frisch MJ, Trucks GW, Schlegel HB, Scuseria GE, Robb MA, Cheeseman JR, Scalmani G, Lee C, Yang W and Parr RG (1988). Development of the Colic-Salvetti correlation-energy formula into a functional of the electron density. *Physical Review* **37(2)**, 785-789.

Halpern J (1965). Catalysis by coordination compounds, *Annu. Rev. Phys. Chem.***16**, 103.

Honzicek J, Vinklarek J, Erben M, Cisarova I (2004). l-Oxo-bis[azidobis(η[5] cyclopentadienyl)-titanium(IV)] *Acta Crystallographica* **60** 1090–1091.

Ibrahim MS and Etaiw dH SE (2004). N,O-Bidentate schiff bases as novel ligands and self-assembled three-dimensional supramolecular complex of silver(i) syntheses and characterization *Synthesis and Reactivity in Inorganic and Metal-Organic Chemistry* **34** 629–639.

Joshi S, Pawar V, Uma V (2011). Synthesis, characterization and biological studies of Schiff bases metal complexes Co(II), Zn (II), Ni (II), and Mn (II) derived from amoxicillin trihydrate with various aldehydes. *International Journal of Pharma and Bio Science* **2** 0975-6299.

Janiak C and Schumann H (1991). Bulky or supracyclopentadienyl derivatives in organometallic chemistry *Adv. Organomet. Chem.* **33** 291.

Jeffery GH, Bassett J, Mendham J, Denny RC, Vogel AI (1989) Textbook of Quantitative Inorganic Analysis, fifth ed. **470.**

Kumar U and Chandra S (2011). Synthesis, spectral and antifungal studies of some coordination compounds of Co(II) andCu(II) of a novel 18-membered octaaza [N8] tetradentate macrocyclic ligand *Journal of Saudi Chemical Society* **15** 19.

Lever ABP (1984). Inorganic Electronic Spectroscopy *2nd Edition.*

Mehrotra R, Shukla SN and Gaur P (2015) Synthesis and spectroscopic characterization of antibacterial rhodium and ruthenium organometallics molded by C–H activation at the ortho position of a phenyl ring *Journal of Coordination Chemistry* **68** 650-661.

Research Article

Mishra M, Tiwari K, Mourya P, Singh MM, Singh VP (2015). Synthesis, characterization and corrosion inhibition property of Ni(II) and Cu(II) complexes with some acylhydrazine Schiff bases *Polyhedron* **89** 29–38.

Mulliken RS (1955). Electronic population analysis on LCAO-MO molecular wave functions. *Journal of Chemical Physics* **23**(10) 1833-1840.

Redd AE,Weinstock RB, Weinhold F (1985). Natural population analysis *Journal of Chemical Physics* **83,** 735-746.

Silverstein RM, Bassler GC and Morrill TC (1991). Spectrometric Identification of Organic Compound. (John Wiley and Sons, Inc) New York 82-108, 123-131, 219-262.

Sujamol MS, Athira CJ, Sindhu Y and Mohanan K (2010). Synthesis, spectroscopic characterization, electrochemical behaviour and thermal decomposition studies of some transition metal complexes with an azo derivative. *Spectrochimica Acta, Part A* **75** 106-112.